Heliyon 9 (2023) e22805

Contents lists available at ScienceDirect

Heliyon

journal homepage: www.cell.com/heliyon

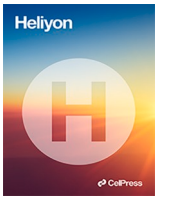

Heat stress suppresses MnSOD expression via p53-Sp1 interaction and induces oxidative stress damage in endothelial cells: Protective effects of MitoQ10 and Pifithrin-α

Jian Gong [a,b,1], Peipei Sun [b,1], Li Li [c,d], Zhimin Zou [c,d], Qihua Wu [b], Liyun Sun [b], Hui Li [a,e], Zhengtao Gu [c,d,**], Lei Su [a,e,*]

[a] Department of Critical Care Medicine, The First School of Clinical Medicine, Southern Medical University (General Hospital of Southern Theater Command of PLA), Guangzhou, 510515, China
[b] Department of Intensive Care Medicine, The Third People's Hospital of Longgang District, Shenzhen, 518115, China
[c] Department of Treatment Center for Traumatic Injuries, The Third Affiliated Hospital of Southern Medical University, Guangzhou, 510630, China
[d] Academy of Orthopedics, Guangdong Province, Guangdong Provincial Key Laboratory of Bone and Joint Degenerative Diseases, The Third Affiliated Hospital of Southern Medical University, Guangzhou, 510630, China
[e] Key Laboratory of Hot Zone Trauma Care and Tissue Repair of PLA, Guangzhou, 510515, China

ARTICLE INFO

Keywords:
Heat stress
Endothelial cells
Oxidative stress
Manganese superoxide dismutase
p53

ABSTRACT

Aim: To investigate the mechanism of p53-mediated suppression of heat stress-induced oxidative stress damage by manganese superoxide dismutase (MnSOD) in endothelial cells (ECs).
Methods: Primary ECs isolated from mouse aortas were used to examine the effects of heat stress on vascular ECs viability and apoptosis. We measured MnSOD expression, reactive oxygen species (ROS) production, p53 expression, viability, and apoptosis of heat stress-induced ECs. We also tested the protective effects of MitoQ10, a mitochondrial-targeted antioxidant, and Pifithrin-α, a p53 inhibitor, in ECs from a mouse model of heat stroke.
Results: Heat stress increased cellular apoptosis, ROS production, and p53 expression, while reducing cellular viability and MnSOD expression in ECs. We also showed that the suppression of MnSOD expression by heat stress in ECs was mediated by interactions between p53 and Sp1. Furthermore, MitoQ10 and Pifithrin-α alleviated heat stress-induced oxidative stress and apoptosis in ECs.
Conclusion: Our results revealed that p53-mediated MnSOD downregulation is a key mechanism for heat stress-induced oxidative stress damage in ECs and indicated that MitoQ10 and Pifithrin-α could be potential therapeutic agents for heat stroke.

* Corresponding author. Department of Critical Care Medicine, The First School of Clinical Medicine, Southern Medical University (General Hospital of Southern Theater Command of PLA); Key Laboratory of Hot Zone Trauma Care and Tissue Repair of PLA, No. 1023, South Shatai Road, Baiyun District, Guangzhou, Guangdong, 510515, China.
** Corresponding author. Department of Treatment Center for Traumatic Injuries, The Third Affiliated Hospital of Southern Medical University; Academy of Orthopedics, Guangdong Province, Guangdong Provincial Key Laboratory of Bone and Joint Degenerative Diseases, The Third Affiliated Hospital of Southern Medical University, No. 183, West Zhongshan Avenue, Tianhe District, Guangzhou, Guangdong, 510630, China.
E-mail addresses: yytao700@smu.edu.cn (Z. Gu), sulei_icu@163.com (L. Su).
[1] These authors contributed equally.

https://doi.org/10.1016/j.heliyon.2023.e22805
Received 21 July 2023; Received in revised form 20 November 2023; Accepted 20 November 2023
Available online 24 November 2023

1. Introduction

Heat-related deaths, including those caused by heatstroke, have increased over the past two decades owing to record-breaking heatwaves [1]. Heatstroke is a life-threatening condition that occurs when the body's core temperature exceeds 40.5 °C as a result of extreme environmental heat exposure. It is characterized by symptoms such as confusion, seizures, and coma. Heatstroke is caused by failure of the body's thermoregulatory mechanisms to maintain cellular and molecular homeostasis. Cardiovascular disease (CVD) is the leading cause of death during heat waves, affecting nearly half a billion people worldwide [2]. A recent study reported that CVD-related mortality increased with every 1 °C rise in temperature across all diagnoses [3].

Heat stroke is associated with vascular endothelial dysfunction [1]. Studies have shown that vascular endothelium becomes discontinuous and apoptotic under heat stress, thereby compromising its barrier function [4]. Oxidative stress is a potential mechanism underlying heat stress-induced endothelial cell apoptosis. Oxidative stress occurs when the production of reactive oxygen species (ROS) exceeds the antioxidant capacity of cells. As previously demonstrated, heat stress can stimulate ROS production, which in turn can activate mitochondrial apoptotic pathways in human umbilical vein endothelial cells [5].

Manganese superoxide dismutase (MnSOD) is the primary antioxidant enzyme in mammalian cells and is responsible for the detoxification of free superoxide radicals [6,7]. It plays a critical role in protecting cells from oxidative stress and in maintaining cellular physiology under genotoxic conditions. However, heat stress significantly reduces MnSOD expression in endothelial cells (ECs) at both mRNA and protein levels, although the underlying mechanisms remain unclear [5]. p53, a well-known tumor suppressor and transcription factor involved in the regulation of oxidative stress, has been implicated in the suppression of MnSOD [8]. It forms a complex with Specificity protein 1 (Sp1), inhibiting *MnSOD* gene transcription under basal and 12-*O*-tetradecanoylphorbol-13-acetate-stimulated conditions [9]. P53 exhibits contrasting roles in oxidative stress regulation, with the ability to either promote oxidative injury through cell cycle arrest, apoptosis, and DNA repair or alleviate oxidative stress by activating antioxidant pathways [10].

MitoQ10 is a lipophilic antioxidant comprising ubiquinol and triphenylphosphonium cation [11]. It specifically accumulates in the mitochondria, where it is converted to its active form and prevents lipid peroxidation and mitochondrial damage. This orally bioavailable compound has demonstrated protective effects against tissue damage and oxidative stress in various disease models such as hypertension, cardiac hypertrophy, and liver cirrhosis.

Hence, the purpose of this study was to investigate the mechanism of p53 mediated MnSOD suppression during heat stress- and oxidative stress-induced damage in ECs.

2. Materials and methods

2.1. Reagents and antibodies

Primary antibodies against GAPDH were purchased from Proteintech (Beijing, China). Primary antibodies against SOD2, p53, and SP1 were purchased from Abcam (Cambridge, UK). iRNA-FITC, puromycin dihydrochloride, hygromycin B, and blasticidin S HCl were purchased from Santa Cruz Biotechnology (Dallas, TX, USA). Mitoquinone mesylate (MitoQ10) and Pifithrin-α, were purchased from Selleck Chemicals (USA). MitoSOX Red Mitochondrial Superoxide Indicator was purchased from Thermo Fisher Scientific (USA).

2.2. Murine heat stress model

The animal surgical procedures followed the National Institutes of Health guidelines and were approved by the Institutional Animal Care and Use Committee of Southern Medical University (License No. SCXK-2011-0015, Guangzhou, Guangdong, China). Pathogen-free 8-week-old male C57BL/6J mice (22–25 g) were purchased from the Experimental Animal Center of the Southern Medical University in Guangzhou. Animals were housed individually at 24 °C with a 12-h diurnal cycle and provided with food and water ad libitum.

Before treatment, the mice were fasted for 12 h but were allowed water ad libitum. As previously described [12], mice in the heat stress group (n = 12) were exposed to a pre-warmed incubator at 35.5 ± 0.5 °C and 60 ± 5 % humidity until severe heat stroke criteria (rectal temperature >43 °C, monitored every 15 min) was achieved. The cells were rewarmed for 6 h. Mice in the control group (n = 12) were sham heated to a temperature of 25 ± 0.5 °C and a humidity of 35 ± 5 % for a comparable duration. To alleviate the impact of heat stress, some mice received MitoQ10 500 μM/day or Pifithrin-α 3 mg/kg prior to heat shock, while saline served as the control. The core body temperatures of the mice were measured using a rectal thermometer before and after heat exposure. At the end of the experiment, the mice were euthanized by cervical dislocation, and their aorta, liver, kidney, heart, and intestinal tissues were harvested and fixed in 4 % paraformaldehyde for further analysis.

2.3. Primary cell isolation, culture, and in vitro models for heat stress

Under sterile conditions, the mouse thoracic aorta was isolated, and the surrounding adipose and connective tissues were carefully dissected and washed repeatedly. Next, the aorta was cut into 1 mm × 1 mm tissue fragments and placed in a culture flask with the intima side facing down. After a 30-min incubation, 2 mL of endothelial culture medium containing basal medium, serum, endothelial growth factor, and penicillin G/streptomycin in a ratio of 100:10:1:1 was gently added to the culture. The cells were then left undisturbed for 3–4 days to allow endothelial cell migration. The tissue fragments were removed, and the cells were used between passages 5 and 8 [13].

Mouse aorta endothelial cells (MAECs) were cultured at a density of 1.0 × 10^5/mL and divided into control and heat-shock groups [12]. The control group was incubated at 37 °C, while the heat shock group was subjected to 43 °C for 2 h. After heat shock, the cells were transferred to a 37 °C incubator for rewarming at different time points (1, 3, 6, and 9 h).

2.4. RNA isolation, cDNA preparation, and quantitative real time polymerase chain reaction (qRT-PCR)

RNA was extracted from cultured cells using TRIzol® (Invitrogen, USA), and cDNA was synthesized with HiScript® III 1st Strand cDNA Synthesis Kit (Vazyme, China). Real-time PCR was performed using the ChamQ Universal SYBR qPCR Master Mix (Vazyme) with *Gapdh* as the control housekeeping gene. The primers used for different target mRNA were as follows: mouse *Sod-2* (Forward: 5′-CCGAGGAGAAGTACCACGAG -3′, Reverse: 5′- GCTTGATAGCCTCCAGCAAC -3'), mouse *Tp53* (Forward: 5′-CCTCATCCTCCTCCTTCCCAGCAG -3′, Reverse: 5′- AACAGATCGTCCATGCAGTGAGGTG -3′), mouse *Sp1* (Forward: 5′- GCTATGC-CAAACCTACTCC -3′, Reverse: 5′- CTGTAGCCCACTGACCCT -3′), and mouse *Gapdh* (Forward: 5′- CAATGTGTCCGTCGTGGATCT -3′, Reverse: 5′- GTCCTCAGTGTAGCCCAAGATG -3′). Three independent experiments were performed.

2.5. Western blotting

The cells were lysed in RIPA buffer containing benzonase, sodium orthovanadate, and protease inhibitors. Protein concentrations were determined using a BCA Protein Assay Kit (Pierce, Rockford, IL, USA). After separating 10–15 μg of protein on 8%–12 % SDS-PAGE gels (Bio-Rad, USA), the proteins were transferred to 0.45 μm PVDF membranes (Bio-Rad). Following blocking with 5 % BSA in TBST, membranes were incubated overnight at 4 °C with primary antibody, then with HRP-linked secondary antibody. Protein bands were visualized using ECL Plus (Millipore, USA) and analyzed using AlphaEase FC Software (Alpha Innotech Corporation, USA). Three independent experiments were performed.

2.6. Cell viability and apoptosis assay

Cell viability and apoptosis were assessed using the ApoTox-Glo™ Triplex Assay kit (Promega, G6320) in 96-well cell cultures. Cells were treated with reaction substrate or control carrier (100 μL), incubated at 37 °C and 5 % CO2. After 1, 3, 6, and 9 h, 20 μL of Viability/Cytotoxicity Reagent (containing GF-AFC Substrate and bis-AAF-R110 Substrate) was added to each well and incubated for 30 min. The fluorescence was measured at 400 nm (excitation) and 505 nm (emission) using a microplate reader. Apoptosis was detected by adding 100 μL of Caspase-Glo® 3/7 Reagent to each well, followed by incubation at room temperature for 30 min, after which luminescence was measured. Three independent experiments were performed.

2.7. Mitochondrial ROS measurement assay, plasma ROS measurement assay, and dihydroethidium staining

A mitochondrial ROS assay kit (Molecular Probes) was used according to the manufacturer's instructions [5]. Detection buffer (120 μL) was added to the cell well, followed by mitochondrial ROS detection reaction solution (100 μL) and incubation for 20 min at 37 °C. The reaction solution was removed and the cells were washed three times with preheated HBSS (120 μL each time). The absorbance values were measured at 480–515 nm (excitation) and 560–600 nm (emission).

Plasma ROS levels were measured according to the manufacturer's protocol (Bioesn). Briefly, 100 L of fresh plasma sample and 10–20 L of O13 probe working solution were added to a 96-well plate, and the pipettes were mixed well. After incubation for 15–30 min at 37 °C, protected from light, the samples were placed in a microplate reader for fluorescence intensity detection (excitation: 516 nm; emission: 606 nm).

Dihydroethidium (DHE) was used to label ROS in the heat-stressed MAECs. Single-cell suspensions (approximately 3 × 10^5 MAECs) and arterial tissues were homogenized and resuspended in cold PBS [13]. Following the kit instructions (Molecular Probes), an appropriate volume of DHE probe was added, and cells were incubated at 37 °C for 30 min in the dark. Fluorescence intensity was measured using flow cytometry with an FL-1 detector (excitation: 353 nm, emission: 515 nm) and corrected for autofluorescence using unlabeled cells. To visualize the ROS levels in tissues and cells, cell slides and tissue sections were incubated with a DHE probe and analyzed using a laser scanning confocal microscope. Three independent experiments were performed.

2.8. siRNA-mediated gene silencing and transfection

Scrambled RNA controls (SC-36869, Santa Cruz), *Tp53*-targeted siRNAs (SC-29436, Santa Cruz), and *Sp1* targeted siRNA (sc-29488, Santa Cruz Biotechnology) were transfected into MAECs using Lipofectamine RNAiMAX (Life Technologies). After 18 h, the medium was changed to DMEM with 10 % FBS, and the cells were incubated for an additional 24–72 h.

For lentiviral transduction, MAECs were seeded in 6-well plates at a density of 2 × 10^5 cells per well. Lentiviral particles targeting *Sod2* (sc-423070-LAC, Santa Cruz), *Sp1* (sc-423094-LAC, Santa Cruz), or *Tp53* (sc-423509-LAC, Santa Cruz) were added to 5 μg/mL polybrene in the complete medium. After overnight incubation, stable cells with overexpression were selected using antibiotics puromycin hydrochloride, hygromycin B, and blasticidin S HCl.

2.9. Co-Immunoprecipitation (co-IP)

To identify protein–protein interactions, CoIP on cell lysates was performed using Protein A/G Magnetic Beads (Beyotime, China), according to the manufacturer's instructions. Briefly, MAECs were harvested after heat stress treatment, lysed with ice-cold mild RIPA buffer on a plate for 30 min, and centrifuged at 12,000 rpm for 10 min to remove cell debris. The supernatant was transferred to a new tube for determination of protein concentration using the Lowry protein assay (Bio-Rad). Equal amounts of protein were mixed with the antibodies of interest (anti-p53 or anti-SP1) and incubated at room temperature for 1 h. Meanwhile, 40 μL protein A + G Magnetic Beads were incubated with 1 mg of antibody (IgG, anti-p53, or anti-Sp1). Then equal amount of protein was mixed with the beads-antibody complex and incubated overnight at 4 °C and then washed three times with lysis buffer. After completion of Co-IP, equal

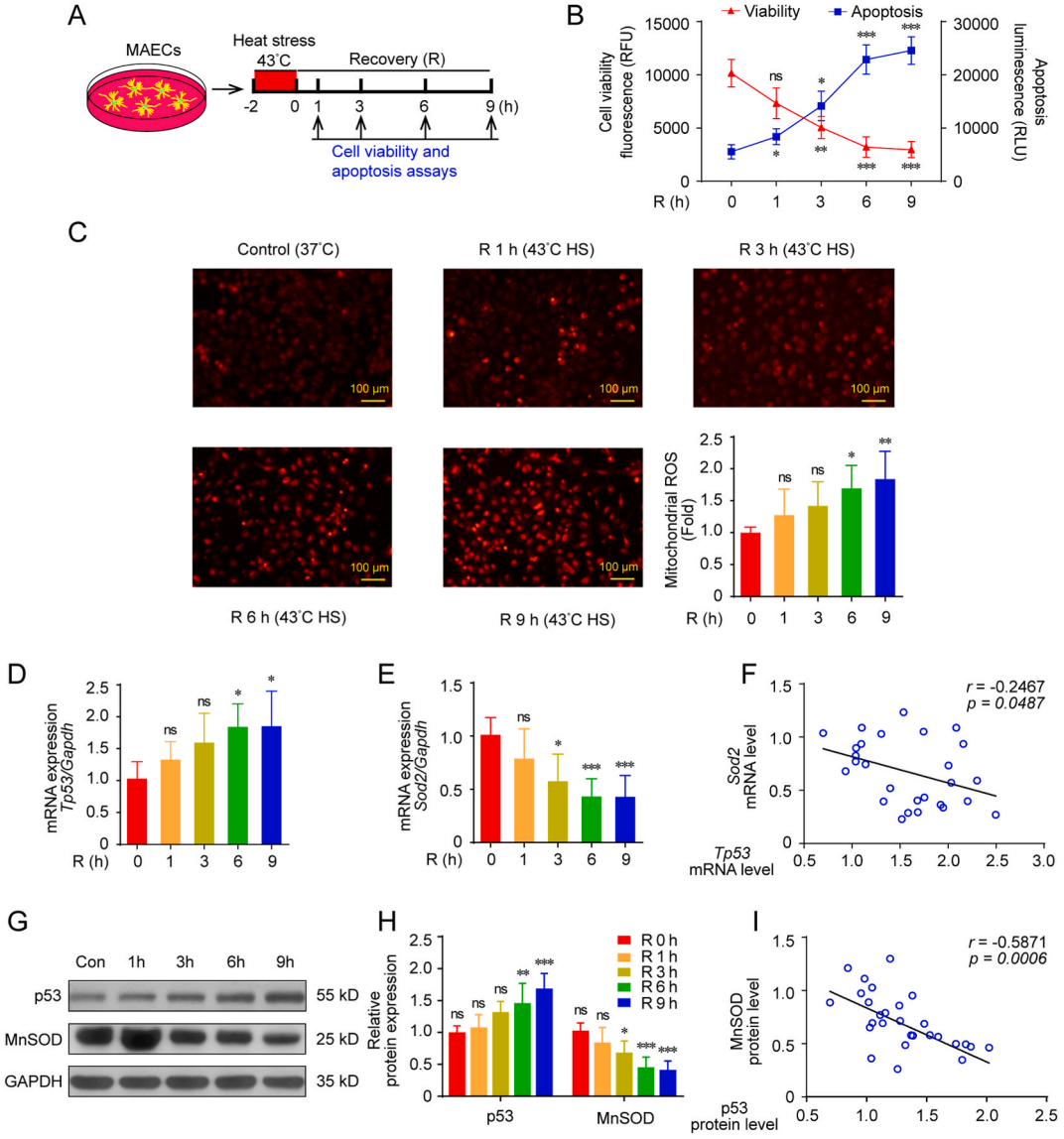

Fig. 1. Heat stress reduces cell viability, increases ROS levels, and upregulates P53 expression while downregulating MnSOD expression **A)** MAECs were exposed to 43 °C for 2 h, then transferred to a 37 °C incubator for rewarming. Cell viability and apoptosis were tested at different time points (1, 3, 6, and 9 h). **B)** Cell viability and apoptosis assay were performed after recovery for 1, 3, 6, and 9 h $^{*}p < 0.05$, $^{**}p < 0.01$, $^{***}p < 0.001$. **C)** Mitochondrial ROS were measured using fluorescent microscope and quantitative analysis was determined using flow cytometry. Scale bar: 100 μm $^{*}p < 0.05$, $^{**}p < 0.01$. **D, E)** The mRNA level of *Tp53* and *Sod2* in MAECs were detected using RT-PCR. $^{*}p < 0.05$. $^{***}p < 0.001$. **F)** The scatter plot showed a negative correlation between the mRNA expression levels of *Tp53* and *Sod2*. The correlation coefficient is −0.2467 and the *p* value is 0.0487. **G)** Protein expression of p53 and MnSOD in MAECs induced by heat stress was detected using western blotting (G) and its grayscale analysis (H) was performed. **I)** The scatter plot displayed a negative correlation between the protein expression levels of p53 and MnSOD. The correlation coefficient is −0.5871 and the *p* value is 0.0006.

sample volumes were analyzed using western blotting, as described previously. Three independent experiments were performed.

2.10. Statistics analysis

Data were presented as mean ± SD and analyzed using SPSS version 21.0 for Windows (IBM Corp). The results were analyzed using Student's t-test or one-way analysis of variance (ANOVA). Multiple comparisons among different groups were performed using the Student–Newman–Keuls (SNK) test after the homogeneity of variance test, with *P < 0.05, **P < 0.01, and ***P < 0.001 considered statistically significant.

3. Results

3.1. Cell viability, apoptosis, and oxidative stress in heat stress-induced MAECs

In response to heat stress stimulation, MAECs were assessed for viability and apoptosis at various time points after recovery from heat stress, as illustrated in Fig. 1A. Fig. 1B shows a significant decrease in cell viability in groups R (3 h), R (6 h), and R (9 h) compared to that in group R (0 h), with no change observed in R (1 h). Furthermore, heat stress treatment resulted in increased apoptosis, as

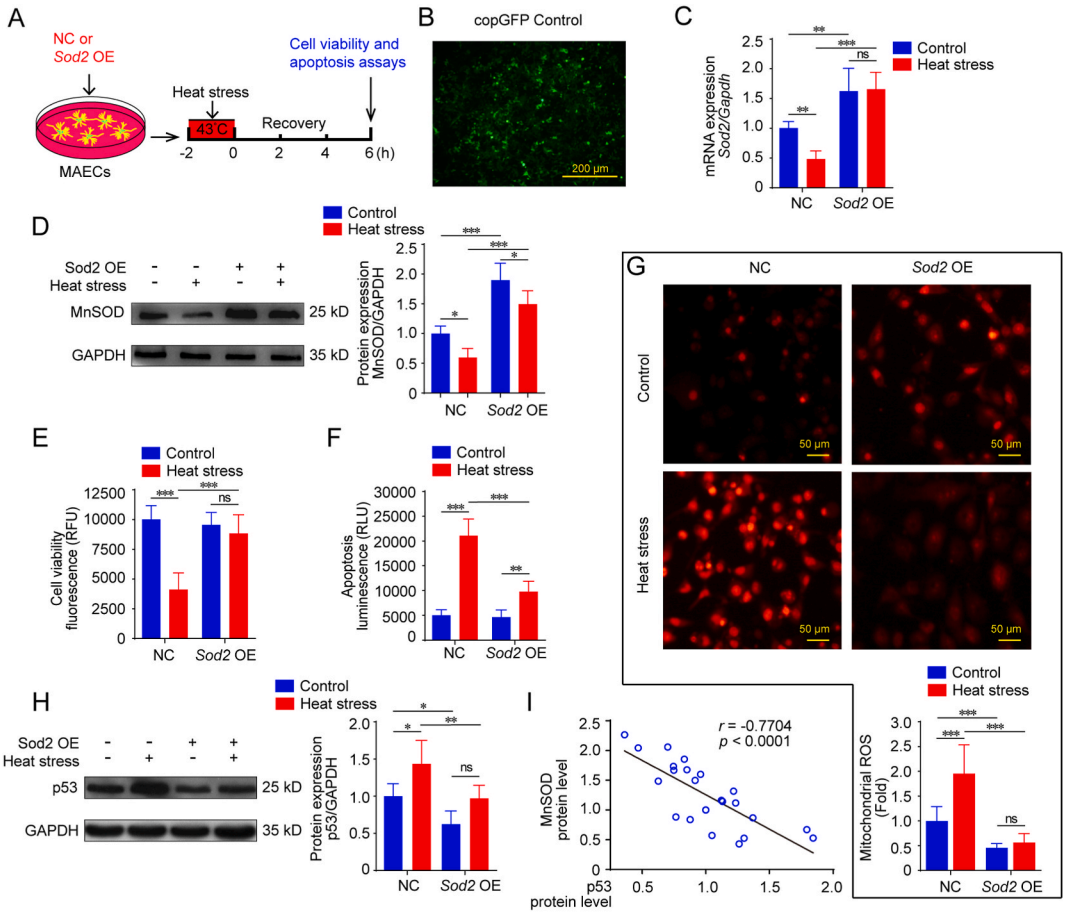

Fig. 2. Overexpression of MnSOD alleviates ROS production and cell damage induced by heat stress **A)** MAECs were transfected with lentivirus targeting *Sod2*, and exposed to 43 °C for 2 h, and subsequently transferred to a 37 °C incubator for rewarming. Cell viability and apoptosis assay were tested after a 6-h recovery period. **B)** The transfection efficiency was validated using copGFP control. Scale bar: 200 μm. **C)** Expression of *Sod2* mRNA was measured using RT-PCR in both control and *Sod2* overexpression groups under normal and heat stress conditions. $^{**}p < 0.01$, $^{***}p < 0.001$. **D)** Expression of MnSOD protein was measured using western blotting in both control and *Sod2* overexpression groups under normal and heat stress conditions. $^{*}p < 0.05$. $^{***}p < 0.001$. **E, F)** Cell viability and apoptosis assay were tested in both control and *Sod2* overexpression groups under normal and heat stress conditions. $^{***}p < 0.001$. **G)** Mitochondrial ROS were visualized using fluorescent microscope and quantitative analysis was determined using flow cytometry. Scale bar: 50 μm $^{***}p < 0.001$. **H)** Expression of p53 protein was measured using western blotting in both control and *Sod2* overexpression groups under normal and heat stress conditions with quantitative analysis performed using greyscale analysis. $^{*}p < 0.05$, $^{**}p < 0.01$. **I)** The scatter plot indicated a negative correlation between the protein expression levels of p53 and MnSOD. The correlation coefficient is −0.7704 and the p value is < 0.0001.

shown in Fig. 1B. Measurement of mitochondrial ROS levels (Fig. 1C) indicated a significant elevation in groups R (6 h) and R (9 h), indicating induction of oxidative stress in heat-stressed MAECs.

3.2. Increased p53 and decreased MnSOD under heat stress

The expression of p53, a well-known tumor suppressor and transcription factor involved in oxidative stress regulation, was significantly increased at both the mRNA (Fig. 1D) and protein levels (Fig. 1G) during R (6 h) and R (9 h). Conversely, the expression of MnSOD, the primary antioxidant enzyme, decreased in groups R (3 h), R (6 h), and R (9 h) (Fig. 1E and G). Notably, a negative correlation was observed between p53 and MnSOD at both mRNA (Fig. 1F) and protein levels (Fig. 1H and I).

3.3. Overexpression of MnSOD alleviates ROS production and cell damage induced by heat stress

To elucidate the role of MnSOD in heat stress-induced oxidative stress, we employed CRISPR-Lentiviral technology to overexpress the *Sod2* gene in MAECs. Subsequently, the cells were subjected to heat stress and allowed to recover in Fig. 2A. The infection

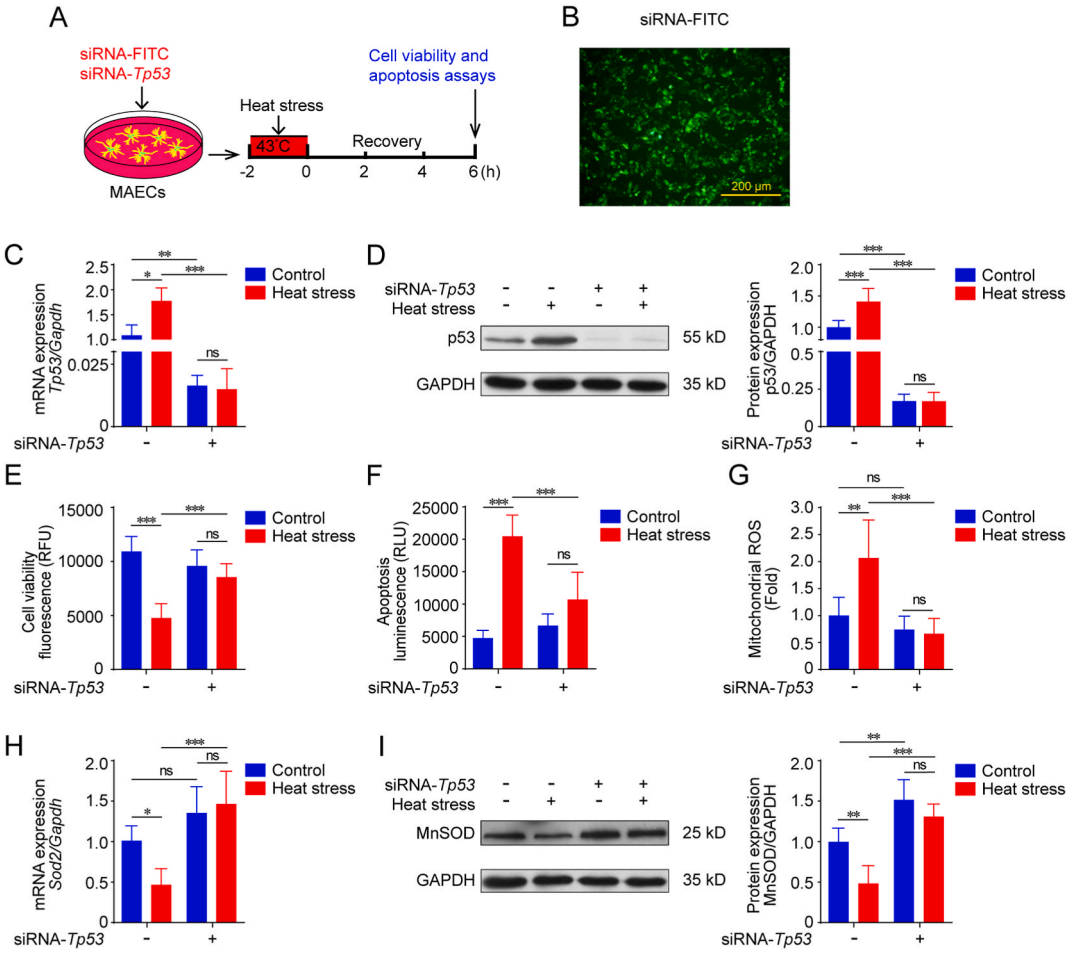

Fig. 3. P53 inhibition mediates the reduction of oxidative stress injury and the increase of MnSOD level in heat stress-induced MAECs A) MAECs were transfected with siRNA targeting *Tp53*, then subjected to 43 °C for 2 h, and subsequently transferred to a 37 °C incubator for rewarming. Cell viability and apoptosis assay were tested after a 6-h recovery period. **B)** The transfection efficiency was validated using siRNA-FITC. Scale bar: 200 μm. **C)** Expression of *Tp53* mRNA was measured using RT-PCR in both control and *Tp53* knockdown groups under normal and heat stress conditions. $^{*}p < 0.05$, $^{**}p < 0.01$, $^{***}p < 0.001$. **D)** Expression of p53 protein was measured using western blotting in both control and p53 knockdown group under normal and heat stress condition (left) with quantitative analysis on the right. $^{***}p < 0.001$. **E, F)** Cell viability and apoptosis assay were tested in both control and *Tp53* knockdown groups under normal and heat stress conditions. $^{***}p < 0.001$. **G)** Mitochondrial ROS level was determined using flow cytometry in both control and *Tp53* knockdown groups under normal and heat stress conditions. $^{**}p < 0.01$, $^{***}p < 0.001$. **H)** Expression of *Sod2* mRNA was measured using RT-PCR in both control and *Tp53* knockdown groups under normal and heat stress conditions. $^{*}p < 0.05$, $^{**}p < 0.01$, $^{***}p < 0.001$. **I)** Expression of p53 protein was measured using western blotting in both control and *Tp53* knockdown groups under normal and heat stress conditions with quantitative results performed using greyscale analysis. $^{**}p < 0.01$, $^{***}p < 0.001$.

efficiency was assessed using a copGFP control (Fig. 2B). The expression analysis of MnSOD at both the mRNA and protein levels in MAECs is presented in Fig. 2C and D. Heat stress led to a significant reduction in MnSOD mRNA expression, which was rescued by *Sod2* overexpression at the mRNA level. Western blot analysis results revealed a significant but attenuated decrease induced by heat stress in the *Sod2* overexpression group (Fig. 2D).

The elevation of *Sod2* conferred a distinct advantage, as evidenced by the amelioration of compromised cell viability and attenuation of heat stress-induced apoptosis, as shown in Fig. 2E and F. Considering the pivotal role of MnSOD in regulating oxidative stress, DHE staining revealed significant attenuation of heat stress-induced mitochondrial ROS with *Sod2* overexpression (Fig. 2G).

Additionally, we evaluated the protein expression of p53 and found that it was reduced in cells overexpressing *Sod2* under both basal and heat stress-induced conditions (Fig. 2H). This finding suggests possible crosstalk between p53 and MnSOD expression (Fig. 2I).

3.4. p53 inhibition mediates the reduction in oxidative stress injury and the increase in MnSOD expression in heat stress-induced MAECs and animal model

To elucidate the possible mechanism by which p53 mediates MnSOD reduction under heat stress, we used siRNA transfection to repress *Tp53* gene expression (Fig. 3A, with siRNA-FITC fluorescence intensity as interference efficiency; Fig. 3B).

In MAECs subjected to heat stress stimulation, the increased expression of p53 was abolished by siRNA targeting *TP53* at both the mRNA (Fig. 3C) and protein levels (Fig. 3D).

Regarding the cellular response to heat stress, siRNA against *TP53* significantly attenuated the heat stress-induced decrease in cell viability (Fig. 3E), increase in apoptosis (Fig. 3F), and mitochondrial ROS production (Fig. 3G). Additionally, PCR and Western blot analyses demonstrated that downregulation of Sod2 and MnSOD in heat-stressed MAECs was inhibited by si*Tp53* (Fig. 3H and I).

To assess the regulating role of p53 *in vivo*, Pifithrin-α, a p53 antagonist, was applied to mice three days before exposure to heat stress (Fig. 4A). Anal temperature remained unchanged with Pifithrin-α treatment (Fig. 4B). As shown in Fig. 4C, Pifithrin-α treatment

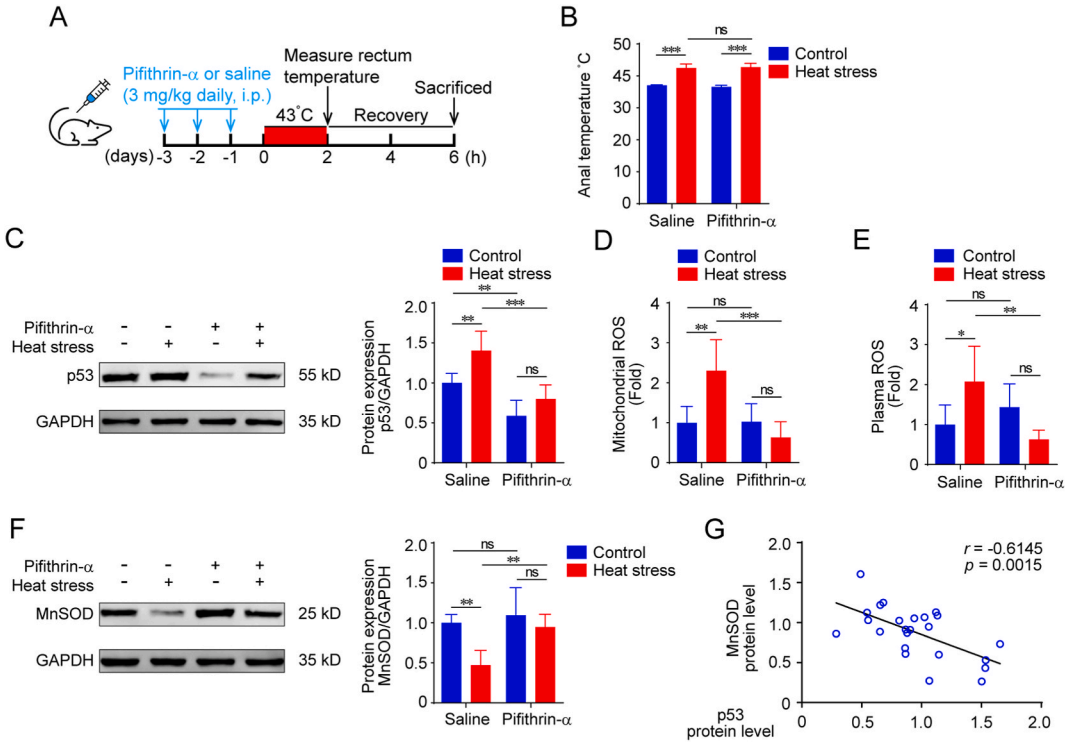

Fig. 4. Inhibition of p53 using Pifithrin attenuated mitochondrial ROS and alleviated MnSOD reduction induced by heat stress **A)** Mice were pretreated with Pifithrin-α (3 mg/kg/day) i. p. for 3 d prior to heat stress treatment. **B)** Rectal temperature was measured in both control and Pifithrin-α treated groups under normal and heat stress conditions. $^{***}p < 0.001$. n = 6 in each group. **C)** Expression of p53 protein was measured using western blotting in both control and Pifithrin-α treated groups under normal and heat stress conditions with quantitative results performed using greyscale analysis. $^{**}p < 0.01$, $^{***}p < 0.001$. **D)** Mitochondrial ROS level was determined using flow cytometry in both control and Pifithrin-α treated groups under normal and heat stress conditions. $^{**}p < 0.01$, $^{***}p < 0.001$. **E)** Plasma ROS was evaluated using a microplate reader in both control and Pifithrin-α treated groups under normal and heat stress conditions. $^{*}p < 0.05$, $^{**}p < 0.01$. **F)** Expression of MnSOD protein was measured using western blotting in both control and Pifithrin-α treated groups under normal and heat stress conditions. $^{**}p < 0.01$, $^{***}p < 0.001$. **G)** The scatter plot indicated a negative correlation between the protein expression levels of p53 and MnSOD. The correlation coefficient is −0.6145 and the *p* value is 0.0015.

significantly reduced p53 expression, inhibiting its sharp elevation during heat stress. Pifithrin-α also reversed the increase in ROS production in both mitochondria and plasma under heat stress (Fig. 4D and E). Heat stress-induced decline in MnSOD expression was abolished by Pifithrin-α pre-treatment (Fig. 4F). Furthermore, there was a negative correlation ($r = -0.6145$, $p = 0.0015$) between p53 and MnSOD at the protein level (Fig. 4G). These findings suggest that p53 mediates oxidative stress injury and MnSOD reduction induced by heat stress both *in vitro* and *in vivo*.

3.5. Oxidative stress injury and MnSOD reduction induced by p53 overexpression in MAECs is not exacerbated under heat stress

To elucidate the role of p53 in heat stress, we utilized CRISPR-Lentiviral to overexpress the *Tp53* gene in MAECs, as depicted in Fig. 5A. The efficacy of transfection and overexpression was validated using a copGFP control (Fig. 5B) and confirmed using the data presented in Fig. 5C.

Interestingly, *Tp53* overexpression had no significant detrimental effects on cell viability (Fig. 5D) in MAECs receiving heat stress treatment and did not induce a significant increase in apoptosis or mitochondrial ROS production (Fig. 5E and F).

Notably, Fig. 5G reveals an intriguing observation: under basal conditions, *Tp53* overexpression led to a decrease in MnSOD expression. However, this decline was not exacerbated by heat stress. These findings suggest that heat stress induces downregulation of MnSOD expression through a mechanism associated with p53 upregulation, which is consistent with the results presented in Fig. 5G.

3.6. Heat stress activates P53 and inhibits SP1 to downregulate MnSOD expression in mouse endothelial cells

To further investigate the mechanism of p53-mediated MnSOD downregulation under heat stress, we manipulated Sp1 expression, a protein known for its interaction with p53 and its involvement in diverse cellular processes, including apoptosis (Fig. 6A). The efficiency and impact of transfection were confirmed (Fig. 6B and C), and a positive correlation between MnSOD and Sp1 expression was observed ($r = 0.8511$, $p = 0.0001$; Fig. 6D). Notably, as shown in Fig. 6E–G, *Sp1* overexpression mitigated heat stress-induced apoptosis, reduced mitochondrial ROS production, and improved cell viability, similar to the effects observed in the heat stress + siRNA-*Tp53* group. Furthermore, the simultaneous knockdown of *Sp1* and *Tp53* exhibited no significant alterations in heat stress-induced apoptosis or mitochondrial ROS. The protein–protein interactions between P53 and Sp1 under heat stress were identified using a co-IP assay (Fig. 6L). Taken together, these findings underscore the dependency of MnSOD and p53 expression, as well as the cellular response to heat stress in MAECs, on Sp1.

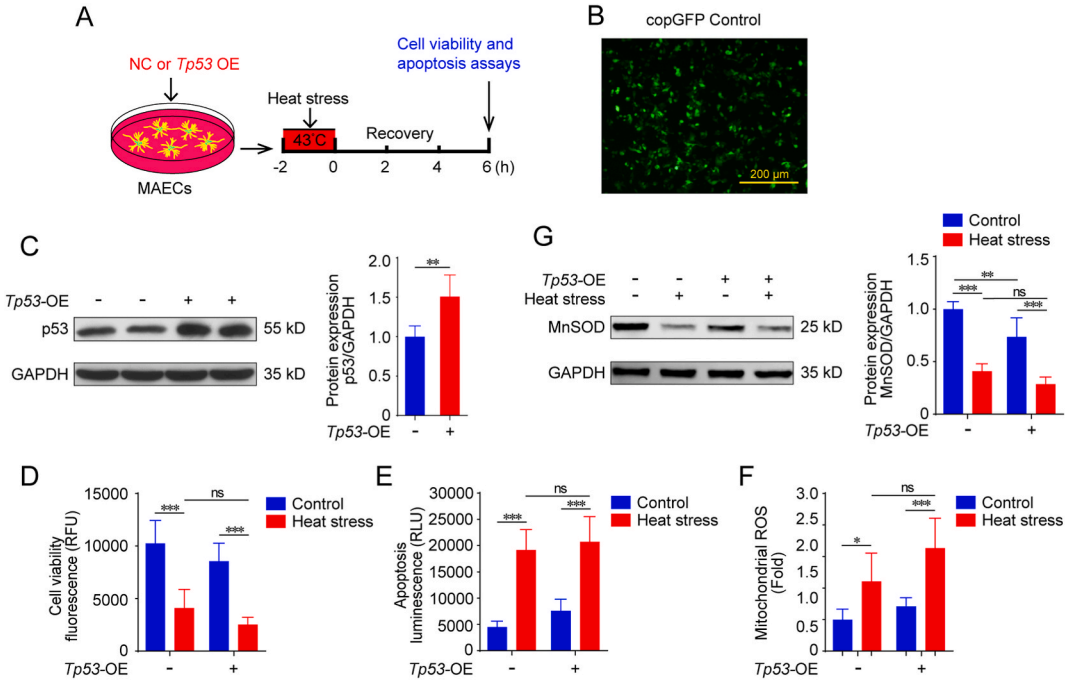

Fig. 5. Oxidative stress Injury and MnSOD Reduction induced by p53 overexpression in MAECs is not exacerbated under heat stress **A)** MAECs were transfected with lentivirus particles targeting *Tp53* prior to heat stress treatment. **B)** Transfection efficiency of lentiviral particles targeting *Tp53* was validated with copGFP control. Scale bar: 200 μm. **C)** The protein overexpression of p53 after transfection was measured using western blotting. $^{**}p < 0.01$. **D, E)** Cell viability and apoptosis assay were tested in both control and *Tp53* overexpression groups under normal and heat stress conditions. $^{***}p < 0.001$. **F)** Mitochondrial ROS level was determined using flow cytometry in both control and *Tp53* overexpression groups under normal and heat stress conditions. $^{*}p < 0.05$, $^{***}p < 0.001$. **G)** Expression of MnSOD protein was measured using western blotting in both control and *Tp53* overexpression groups under normal and heat stress conditions. $^{**}p < 0.01$, $^{***}p < 0.001$.

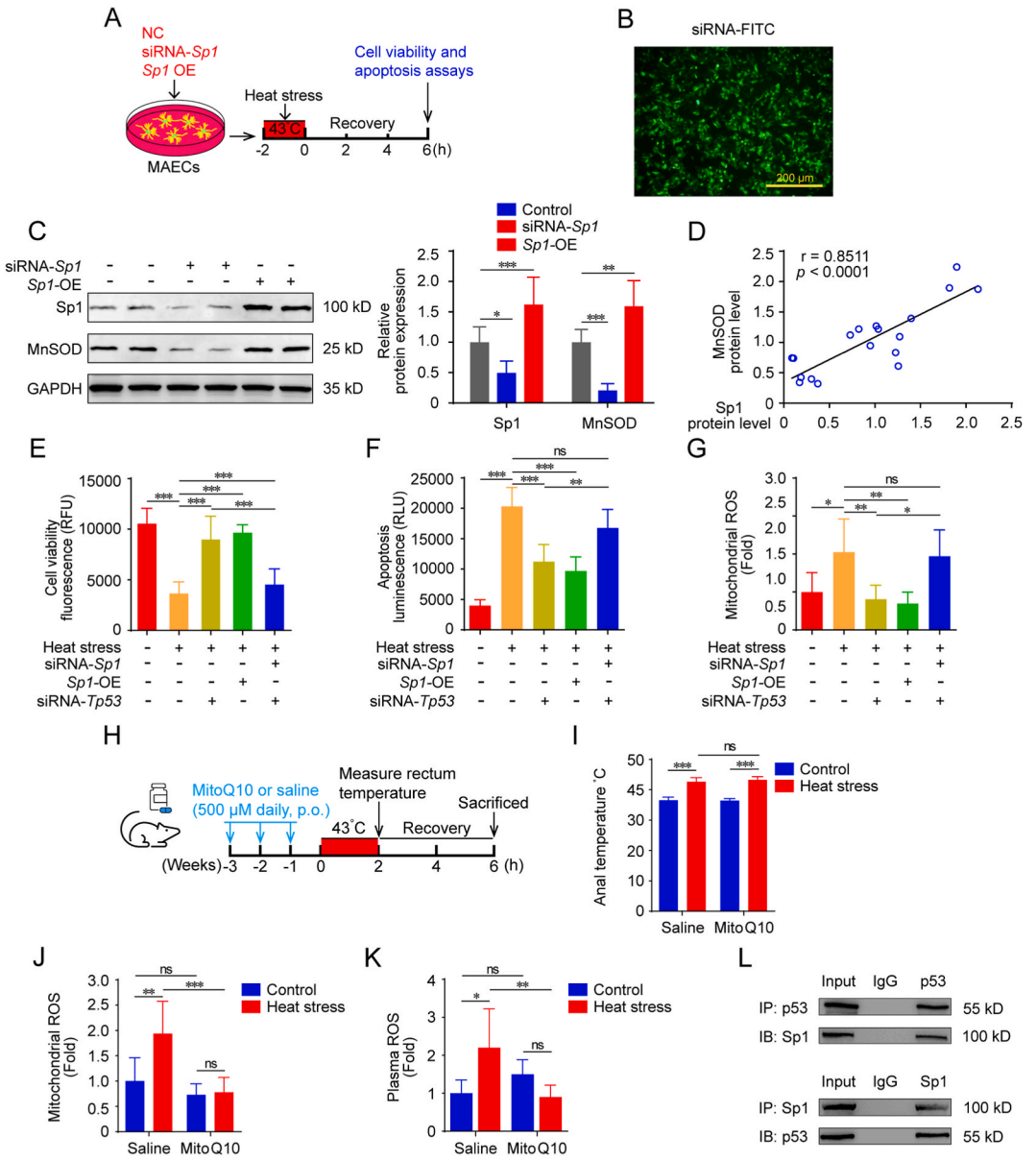

Fig. 6. Heat stress activates p53 and inhibits SP1 to downregulate MnSOD expression in mouse endothelial cells **A)** MAECs were transfected with siRNA targeting *Sp1* and *Tp53*, or lentivirus particles targeting *Sp1* prior to heat stress treatment. **B)** The transfection efficiency was validated using siRNA-FITC. Scale bar: 200 μm. **C)** The expression of Sp1 protein in both Sp1 knockdown and overexpression groups using western blotting. $^{*}p < 0.05$, $^{**}p < 0.01$, $^{***}p < 0.001$. **D)** The scatter plot showed a positive correlation between the protein expression levels of Sp1 and MnSOD. The correlation coefficient is 0.8511 and *p*-value is < 0.0001. **E, F)** Cell viability and apoptosis assay were tested in control, siRNA-*Tp53*, *SP1* overexpression, and siRNA-*Tp53-Sp1* groups under heat stress conditions. $^{**}p < 0.01$, $^{***}p < 0.001$. **G)** Mitochondrial ROS level was determined using flow cytometry in control, siRNA-*Tp53*, *SP1* overexpression, and siRNA-*Tp53-Sp1* groups under heat stress conditions. $^{*}p < 0.05$, $^{**}p < 0.01$. **H)** Mice were treated with MitoQ10 (500 μM/day) or saline 3 weeks prior to heat stress. **I)** Rectal temperature was measured in both control and MitoQ10 treated groups under normal and heat stress conditions. $^{***}p < 0.001$. n = 6 in each group. **J)** Mitochondrial ROS level was determined using flow cytometry in both control and MitoQ10 treated groups under normal and heat stress conditions. $^{**}p < 0.01$, $^{***}p < 0.001$. **K)** The measurement of Plasma ROS was conducted by a microplate reader in both control and MitoQ10 treated groups under normal and heat stress conditions. $^{*}p < 0.05$, $^{**}p < 0.01$. **L):** P53 interacts with Sp1 in co-IP assays in MAECs incubated under heat stress conditions.

3.7. Antioxidant alleviates the ROS level in heat stress treated mice

To investigate the therapeutic potential of an antioxidant in heat stress, we administered MitoQ10 to mice for three weeks prior to heat stress treatment. Notably, MitoQ10-treated mice exhibited no alteration in core body temperature, as measured by rectal

temperature, following heat stress (Fig. 6H and I).

As depicted in Fig. 6J and K, heat stress stimulation significantly elevated the levels of mitochondrial and plasma ROS in mice, whereas treatment with MitoQ10 significantly attenuated these trends. These findings highlight the promising therapeutic effects of MitoQ10 in the amelioration of heat stress-induced oxidative stress.

4. Discussion

Exposure to hot conditions increases stress on the cardiovascular system, leading to higher morbidity and mortality, especially considering that global temperatures have risen by 0.99 °C in the first two decades of the 21st century [14,15]. Increased cell temperatures disrupt vital cellular processes, causing apoptosis and reducing cell viability [16,17]. Apoptosis is an important factor in the development of diseases caused by heat stress [18]. Our study evaluated endothelial cell damage during the acute phase response to heat stress and showed significant induction of apoptosis in primary MAECs.

During heat stress, we observed an increase in ROS levels. While ROS play a crucial role in cellular signaling, excessive ROS and reactive nitrogen species concentrations result in uncontrolled free radical-mediated chain reactions, causing damage to proteins, lipids, polysaccharides, and DNA and triggering the intrinsic apoptotic pathway [4,19]. Heat stress induces ROS overproduction, partly due to the downregulation of antioxidant enzymes, such as MnSOD, as observed in our results. MnSODs protect cells against the cytotoxic effects of heat stress [20]. However, MnSOD alone may be insufficient to prevent oxidative damage. It works in conjunction with glutathione peroxidase (GSPx) and glutathione (GSH) for the complete detoxification of H_2O_2. Heat stress reduces both SOD and GSH levels, resulting in increased H_2O_2 that can diffuse freely across cell membranes because of its small size and relatively low reactivity, causing toxic effects far from the site of ROS production [7]. In addition to MnSOD, heat stress decreases cytoplasmic SOD protein and enzyme activities, leading to increased ROS production and superoxide dismutase 1 mRNA levels [6]. A previous study revealed that MnSOD overexpression in breast cancer cells downregulated p53 promoter activity in an NF-κB-independent manner [21]. While these findings offer insights, further investigation of endothelial cells is needed to better understand MnSOD-p53 interactions, particularly under heat-stress conditions.

Mitoquinone mesylate (MitoQ10) is a mitochondrially targeted antioxidant that protects against oxidative damage [22]. In our *in vivo* study, MitoQ10 treatment significantly reduced mitochondrial and plasma ROS levels. Recently, this antioxidant was used to attenuate PM2.5-induced vascular fibrosis by regulating mitophagy [23]. Clinical trials are required to investigate the protective effects of MitoQ10 over heat stroke.

p53 is a tumor suppressor that regulates various signaling pathways [8]. In both our *in vivo* and *in vitro* analyses, p53 expression was elevated and negatively associated with MnSOD under heat-stress conditions. The enhanced cell apoptosis during heat stress in the group with downregulated expression using siRNA or inhibited transcriptional activity of p53 with Pifithrin-α can be attributed to impaired MnSOD expression. However, p53 overexpression does not promote these cellular processes. These findings suggest that p53 plays a complex role in mediating the oxidative stress burden, depending on the specific properties of the stress applied, as indicated by previous studies. Under low to moderate oxidative stress, p53 activates pathways that increase cell repair time, such as cell cycle arrest and autophagy, to enhance cell survival [24,25]. However, under intense and prolonged stress caused by factors such as irradiation, hypoxia, or oxidizing agents, p53 switches to facilitate increased cellular stress levels by inducing DNA fragmentation, resulting in apoptosis and prevention of cell proliferation.

To investigate the mechanism by which p53 mediates MnSOD activity during heat stress, we examined the role of Sp1, a key transcription factor for MnSOD that interacts with p53 [26]. As depicted in Fig. 6, Sp1 acts as a protective factor by reducing cell apoptosis and mitochondrial ROS levels under heat stress. Additionally, it positively influenced MnSOD transcription under constitutive conditions. In our study, inhibiting expression of Sp1 resulted in increased apoptosis and mitochondrial ROS levels during heat stress. However, when p53 expression was inhibited, these effects were reversed. These findings are consistent with those of a well-established study [9], suggesting a regulatory role for p53 in both basal and induced MnSOD gene transcription by interfering with the transcriptional machinery. Moreover, as shown in this study, a complex was formed between P53 and Sp1 under basal conditions [24]. Indeed, our co-IP confirmed the existence of this complex under heat stress. Formation of a complex between p53 and Sp1 in the promoter region is likely to have a significant impact on MnSOD production in response to oxidative stress.

This study had some limitations that should be acknowledged. We used only one cell line and one animal model to study the effects of heat stress, which may limit the generalizability of our findings to other cell types and species. In addition, we did not investigate the effects of different heat stress durations and intensities on p53 and MnSOD expression and activity in MAECs and animal models, which may provide more insight into the dose-response relationship between heat stress and oxidative stress injury.

In conclusion, our study demonstrated that heat stress induces oxidative stress injury and cell viability impairment in MAECs and animal models, and that these effects are mediated by p53 and MnSOD. Moreover, p53 upregulation and MnSOD downregulation are dependent on the Sp1 transcription factor, and manipulation of the expression of these genes can modulate the cellular response to heat stress. This study provides new insights into the molecular mechanisms of heat stress-induced oxidative stress injury and identifies potential therapeutic targets for heatstroke. However, further studies are required to explore the downstream signaling pathways.

Ethics statement

This study was approved and supervised by the Laboratory Animal Ethics Committee of General Hospital of Southern Theater Command of PLA (approval number: 2019123101).

Consent for publication

All authors Consent for publication.

Author contribution statement

L.S, J.G, and Z.T.G performed the study and composed this manuscript. Q.H.W and P.P.S. were responsible for primary data generation and analysis. P.P.S, J.G. and L.L. participated in animal modeling and cell culture. Z.M.Z and H.L. Performed transfection and Weston blots. L.S. and Z.T.G. was the principal investigator and corresponding author for these studies.

Data availability statement

No data associated with our study been deposited into a publicly available repository. And data will be made available on request.

Additional information

No additional information is available for this paper.

Declaration of competing interest

The authors declare the following financial interests/personal relationships which may be considered as potential competing interests:Jian Gong reports financial support was provided by Shenzhen City Science and Technology Planning Project of Guangdong Province (JCYJ20180228162214347). Jian Gong reports financial support was provided by Special fund for economic and technological development of Longgang District, Shenzhen city Medical and health science and technology program projects (LGWJ2021148). If there are other authors, they declare that they have no known competing financial interests or personal relationships that could have appeared to influence the work reported in this paper.

Acknowledgments

This study was supported by the Shenzhen City Science and Technology Planning Project of Guangdong Province (JCYJ20180228162214347), special fund for economic and technological development of Longgang District, and Shenzhen city Medical and health science and technology program projects (LGWJ2021148).

References

[1] A. Bouchama, B. Abuyassin, C. Lehe, O. Laitano, O. Jay, F.G. O'Connor, L.R. Leon, Classic and exertional heatstroke, Nat. Rev. Dis. Prim. 8 (2022) 8, https://doi.org/10.1038/s41572-021-00334-6.
[2] J. Ozkan, Too Hot to Handle? the Truth about the Effects of Extreme Heat on Cardiovascular Health, European Heart Journal, 2022, https://doi.org/10.1093/eurheartj/ehac554 ehac554.
[3] K.L. Ebi, A. Capon, P. Berry, C. Broderick, R. de Dear, G. Havenith, Y. Honda, R.S. Kovats, W. Ma, A. Malik, N.B. Morris, L. Nybo, S.I. Seneviratne, J. Vanos, O. Jay, Hot weather and heat extremes: health risks, Lancet 398 (2021) 698–708, https://doi.org/10.1016/S0140-6736(21)01208-3.
[4] F. Y, K. L, W. X, M. D, M. Y, H. Z, Role of iron-related oxidative stress and mitochondrial dysfunction in cardiovascular diseases, Oxid. Med. Cell. Longev. (2022) 2022, https://doi.org/10.1155/2022/5124553.
[5] F. Wu, X.J. Dong, H.Q. Zhang, L. Li, Q.L. Xu, Z.F. Liu, Z.T. Gu, L. Su, Role of MnSOD in propofol protection of human umbilical vein endothelial cells injured by heat stress, J. Anesth. 30 (2016) 410–419, https://doi.org/10.1007/s00540-015-2129-2.
[6] D. Candas, J.J. Li, MnSOD in oxidative stress response-potential regulation *via* mitochondrial protein influx, Antioxidants Redox Signal. 20 (2014) 1599–1617, https://doi.org/10.1089/ars.2013.5305.
[7] B.V. R, The structure-function relationships and physiological roles of MnSOD mutants, Biosci. Rep. 42 (2022), https://doi.org/10.1042/BSR20220202.
[8] B. Lj H, E.-D. Ws, Tumor suppressor p53: biology, signaling pathways, and therapeutic targeting, Biochim. Biophys. Acta, Rev. Cancer (2021) 1876, https://doi.org/10.1016/j.bbcan.2021.188556.
[9] S.K. Dhar, Y. Xu, Y. Chen, D.K. St Clair, Specificity protein 1-dependent p53-mediated suppression of human manganese superoxide dismutase gene expression, J. Biol. Chem. 281 (2006) 21698–21709, https://doi.org/10.1074/jbc.M601083200.
[10] F. Kruiswijk, C. Labuschagne, K. Vousden, p53 in survival, death and metabolic health: a lifeguard with a licence to kill, Nat. Rev. Mol. Cell Biol. 16 (2015) 393–405.
[11] Nm B, J. O, S. Ab, R. Am, A. O, O. R, R. M, S. M, Mitochondrial dysfunction in the cardio-renal Axis, Int. J. Mol. Sci. 24 (2023), https://doi.org/10.3390/ijms24098209.
[12] L. L, Z. Z, Q. L, K. Z, L. S, Z. G, Extranuclear P53 Suppresses Autophagy through AMPK/mTOR Signaling to Promote Heat Stress-Induced Vascular Endothelial Cell Damage, Nan Fang Yi Ke Da Xue Xue Bao, vol. 41, Journal of Southern Medical University, 2021, https://doi.org/10.12122/j.issn.1673-4254.2021.11.10.
[13] M. K, K. I, E. W, T. M, T. K, A simple method of isolating mouse aortic endothelial cells, J. Atherosclerosis Thromb. 12 (2005), https://doi.org/10.5551/jat.12.138.
[14] M. Marchand, K. Gin, The cardiovascular system in heat stroke, CJC Open 4 (2022) 158–163, https://doi.org/10.1016/j.cjco.2021.10.002.
[15] C.G. Crandall, T.E. Wilson, Human cardiovascular responses to passive heat stress, in: R. Terjung (Ed.), Comprehensive Physiology, first ed., Wiley, 2014, pp. 17–43, https://doi.org/10.1002/cphy.c140015.
[16] M.N. Cramer, D. Gagnon, O. Laitano, C.G. Crandall, Human temperature regulation under heat stress in health, disease, and injury, Physiol. Rev. 102 (2022) 1907–1989, https://doi.org/10.1152/physrev.00047.2021.
[17] I. Belhadj Slimen, T. Najar, A. Ghram, H. Dabbebi, M. Ben Mrad, M. Abdrabbah, Reactive oxygen species, heat stress and oxidative-induced mitochondrial damage, A review, International Journal of Hyperthermia. 30 (2014) 513–523, https://doi.org/10.3109/02656736.2014.971446.

[18] W. Huang, W. Xie, J. Gong, W. Wang, S. Cai, Q. Huang, Z. Chen, Y. Liu, Heat stress induces RIP1/RIP3-dependent necroptosis through the MAPK, NF-κB, and c-Jun signaling pathways in pulmonary vascular endothelial cells, Biochem. Biophys. Res. Commun. 528 (2020) 206–212, https://doi.org/10.1016/j.bbrc.2020.04.150.
[19] D. Zheng, J. Liu, H. Piao, Z. Zhu, R. Wei, K. Liu, ROS-triggered endothelial cell death mechanisms: focus on pyroptosis, parthanatos, and ferroptosis, Front. Immunol. 13 (2022), 1039241, https://doi.org/10.3389/fimmu.2022.1039241.
[20] M. L, X. S, B. C, R. D, Z. X, H. X, Insights into manganese superoxide dismutase and human diseases, Int. J. Mol. Sci. 23 (2022), https://doi.org/10.3390/ijms232415893.
[21] P. Drane, A. Bravard, V. Bouvard, E. May, Reciprocal down-regulation of p53 and SOD2 gene expression ± implication in p53 mediated apoptosis, Oncogene 20 (2001) 430–439, https://doi.org/10.1038/sj.onc.1204101.
[22] W. B, H. X, C. S, X. L, H. L, J. M, F. G, Z. D, X. L, Neutrophils restrain sepsis associated coagulopathy via extracellular vesicles carrying superoxide dismutase 2 in a murine model of lipopolysaccharide induced sepsis, Nat. Commun. 13 (2022), https://doi.org/10.1038/s41467-022-32325-w.
[23] C. J, M. Z, H. Z, A. S, Y. J, T. C, PM2.5 induces mitochondrial dysfunction via AHR-mediated cyp1a1 overexpression during zebrafish heart development, Toxicology 487 (2023), https://doi.org/10.1016/j.tox.2023.153466.
[24] X. Liu, L. Fan, C. Lu, S. Yin, H. Hu, Functional role of p53 in the regulation of chemical-induced oxidative stress, 2020, Oxid. Med. Cell. Longev. (2020) 1–10, https://doi.org/10.1155/2020/6039769.
[25] K. Beyfuss, D.A. Hood, A systematic review of p53 regulation of oxidative stress in skeletal muscle, Redox Rep. 23 (2018) 100–117, https://doi.org/10.1080/13510002.2017.1416773.
[26] J.-F. Jiang, Z.-Y. Zhou, Y.-Z. Liu, L. Wu, B.-B. Nie, L. Huang, C. Zhang, Role of Sp1 in atherosclerosis, Mol. Biol. Rep. 49 (2022) 9893–9902, https://doi.org/10.1007/s11033-022-07516-9.